Review of Scientific Instruments | ARTICLE | scitation.org/journal/rsi

A spectrum matching method for accurate frequency estimation of real sinusoids

Cite as: Rev. Sci. Instrum. 90, 045112 (2019); doi: 10.1063/1.5091024
Submitted: 31 January 2019 • Accepted: 20 March 2019 •
Published Online: 10 April 2019

Kui Wang,[1,a)] Yaqing Tu,[1,b)] Des McLernon,[2] Yanlin Shen,[3] and Peng Chen[1]

AFFILIATIONS

[1] Department of Military Logistics, People's Liberation Army Logistical Engineering University, Chongqing 401311, China
[2] School of Electronic and Electrical Engineering, The University of Leeds, Leeds LS2 9JT, United Kingdom
[3] Department of Equipment Support, Logistics University of People's Armed Police Force, Tianjin 300309, China

[a)] **Email:** kuiwang.nudt@hotmail.com
[b)] **Author to whom correspondence should be addressed:** yaqingtu@126.com

ABSTRACT

It is well-known that incoherent sampling is detrimental for frequency estimation of a real sinusoid, and the estimation errors get worse when the signal lengths are very short. In this paper, a spectrum matching based frequency estimator is proposed as well as evaluated against other four two-step methods developed to suppress the effect of incoherent sampling. The spectral interference introduced by incoherent sampling is eliminated via a spectrum matching process including modulation and spectral analysis. A further error correction based on Fourier transform is conducted to generate the fine frequency estimate. Simulation results are carried out to show that the proposed method can closely approach the Cramér-Rao lower bound without any error floor, and it can outperform the other four methods particularly for short signal lengths.

I. INTRODUCTION

Frequency estimation of sinusoids has been a subject of investigation in many fields for decades, such as radar, power systems, measurement, and instrumentation. Numerous estimation approaches have been developed so far. Given a straightforward operation of maximizing the periodogram,[1] frequency domain approaches based on the discrete Fourier transform (DFT) and implemented by the fast Fourier transform (FFT) show high computational efficiency. A typical two-step scheme is widely concerned, which usually includes a coarse estimation via DFT to locate the spectral maximum, followed by a fractional interpolation with two or more spectral points.[2–4] However, a majority of these two-step methods are only adapted to complex signals, and for real sinusoids, the inherent picket fence effect and spectral leakage of the DFT may introduce significant errors if the signal is not coherently sampled.[5,6] In addition, the DFT based methods suffer from resolution loss when the signal lengths are very short.

In time domain, the two-step procedure is also introduced to promote the estimation performance. The two-stage autocorrelation (TSA) approach[7] employs the linear property (LP) to reform the signal and makes use of different lags of autocorrelations to produce frequency estimates. To avoid multiple autocorrelations which are computationally burdensome, the Taylor expansion and the least squares (LS) principle are involved to generate an error function in the extended autocorrelation (EA) method.[8] By minimizing the error function, the performance of the EA method can approach the Cramér-Rao lower bound (CRLB) when the signal lengths are sufficiently large. However, coping with incoherently sampled data in short length, the EA method performs biased significantly because the signal autocorrelation has an error term which is not negligible. Accordingly, the recently proposed phase match (PM) based method[9] and phase correction autocorrelation (PCA) method[10] show different ways of reconstructing the autocorrelation function to avoid the error term, and besides, the Cauchy inequality is also considered to derive the error function in Ref. 9. Generally, the PM and PCA methods are effective to deal with the incoherently sampled signal, but their performance still shows slight degradation when the signal lengths are very short.

In this paper, a new two-step frequency estimator based on spectrum matching is proposed, which shows improvements in accuracy among the aforementioned two-step methods. The estimation bias caused by incoherent sampling is effectively reduced by modulation, which has already been validated in our previous work.[11] Then, spectral analysis is carried out to divide the original signal spectrum into two separated complex versions, which we call spectrum matching. Finally, the fine estimate results from an error correction via a classical approach based on Fourier transform.[12] The rest of this paper is organized as follows: In Sec. II, the underlying principle to deal with the spectral interference caused by incoherent sampling is interpreted. The whole algorithm is carried out in Sec. III. Performance comparison is conducted in Sec. IV, and the final conclusion is presented in Sec. V.

II. UNDERLYING PRINCIPLE

Consider a general, real sinusoid in noise as follows:

$$x(n) = A\cos(\omega_0 n + \theta) + w(n), n = 1, 2, 3, \ldots, N-1, \tag{1}$$

where A and θ represent the signal amplitude and the initial phase, respectively, $\omega_0 (0 < \omega_0 < \pi)$ is the normalized angular frequency in units of radians per sample, and $w(n)$ is the zero-mean additive white Gaussian noise (AWGN) with a variance of σ^2.

From Refs. 9 and 10, we know that if the signal is incoherently sampled, the signal autocorrelation has an error term which is only negligible for sufficiently large N. In frequency domain, the spectrum of the incoherently sampled signal suffers from interference from the negative frequency components, and it gets worse for small values of N. In addition, although the number of samples is increasing, the chosen value of ω_0 will almost surely not exactly coincide with a DFT frequency bin, and so, it is inevitable that we will have to deal with the effect of incoherent sampling for accurate frequency estimation. Now, with *a priori* knowledge of the signal frequency, which is provided by the coarse estimation, the signal frequency can be directly modulated to approach coherent sampling.

Modulate the signal as $x_m(n) = x(n)e^{j\omega_c n}$, and then

$$x_m(n) = (A/2)e^{j((\omega_0+\omega_c)n+\theta)} + (A/2)e^{-j((\omega_0-\omega_c)n+\theta)} + w(n)e^{j\omega_c n}, \tag{2}$$

where ω_c $(0 \le \omega_c \le \omega_0)$ is the modulation frequency.

Calculate the DFT of $x_m(n)$, denoted as $X_m(k)$, as

$$X_m(k) = S_{m+}(k) + S_{m-}(k) + W_m(k), \tag{3}$$

where $W_m(k)$ is the DFT of the modulated noise, $S_{m+}(k)$ and $S_{m-}(k)$ are the DFT of the positive and negative frequency exponentials in (2), respectively, which can be written as

$$\begin{cases} S_{m+}(k) = \dfrac{A}{2}e^{j\theta}e^{j\frac{N-1}{2}(\omega_0+\omega_c-\tilde{\omega}_k)}\dfrac{\sin((\omega_0+\omega_c-\tilde{\omega}_k)N/2)}{\sin((\omega_0+\omega_c-\tilde{\omega}_k)/2)} \\ S_{m-}(k) = \dfrac{A}{2}e^{-j\theta}e^{-j\frac{N-1}{2}(\omega_0-\omega_c+\tilde{\omega}_k)}\dfrac{\sin((\omega_0-\omega_c+\tilde{\omega}_k)N/2)}{\sin((\omega_0-\omega_c+\tilde{\omega}_k)/2)} \end{cases}, \tag{4}$$

where $\tilde{\omega}_k = 2\pi k/N$ represents the kth DFT frequency bin, and $k = 0, 1, 2, \ldots, N-1$.

Note that in (4), we can force most values of $S_{m+}(k)$ or $S_{m-}(k)$ to be zero only by setting $\omega_0 + \omega_c = 2\pi m/N$ or $\omega_0 - \omega_c = 2\pi m/N$ (m is an arbitrary integer). For example, in the absence of noise, if we set $\omega_c = \omega_0$, the modulus of $S_{m+}(k)$ and $S_{m-}(k)$ is shown in Fig. 1

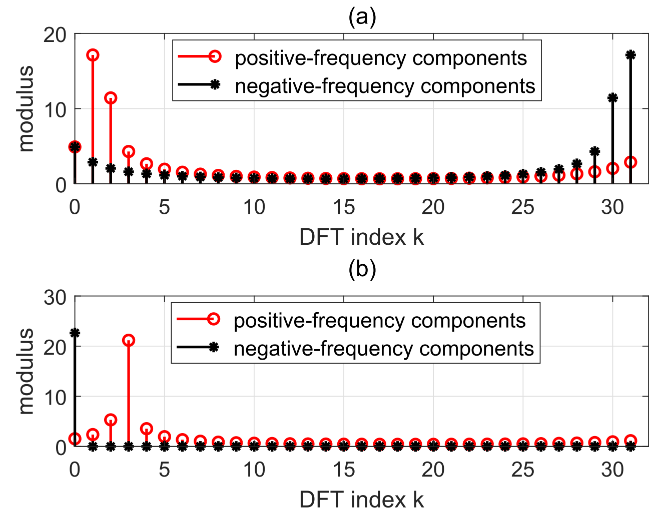

FIG. 1. Interaction of positive and negative frequency components (zero noise), where the DFT index k refers to a normalized angular frequency of $\omega = 2\pi k/N$, $0 \le k \le N-1$. (a) Before modulation and (b) after modulation ($\omega_c = \omega_0$).

($\omega_0 = 0.0876\pi$, $N = 32$, and $\theta = \pi/7$). Serious interference of the negative frequency components occurs in Fig. 1(a), and the frequency estimation which ignores the negative frequency contribution will exhibit a significant bias. But in Fig. 1(b), the negative frequency component has $S_{m-}(k) = 0$ for all values of k excluding $k = 0$, which means the interference only exists at $k = 0$. Thus, if we can figure out $S_{m+}(0)$, it is possible to match $X_m(k)$, which is the spectrum of a real signal, to the spectrum of a complex sinusoid as $S_{m+}(k)$. The spectral interference of the negative frequency components can be eliminated in this case.

III. METHOD DEVELOPMENT

A. Coarse estimation

In practice, ω_0 is unknown and ω_c can only be set according to a coarse frequency estimate $\hat{\omega}_0^c$. Assume $\omega_c = \hat{\omega}_0^c = \omega_0 + \Delta\omega_0^c$, where $\Delta\omega_0^c$ is the estimation error. Then, from (4) for $k = 0, 1, 2, \ldots, N-1$, we get

$$S_{m-}(k) = (-1)^k \frac{A}{2}e^{-j\theta}e^{-j\frac{N-1}{2}(\tilde{\omega}_k-\Delta\omega_0^c)}\frac{\sin(N\Delta\omega_0^c/2)}{\sin((\Delta\omega_0^c-\tilde{\omega}_k)/2)}. \tag{5}$$

Obviously, $S_{m-}(k)$ is proportional to $\sin(N\Delta\omega_0^c/2)$, and $S_{m-}(k) \ne 0$ when $k \ne 0$. Thus, we need $|N\Delta\omega_0^c|$ to be sufficiently small (empirically $|N\Delta\omega_0^c| < 0.1$) so that the interference occurred at $k \ne 0$ can be ignored. To that end, we give an enhanced version of the modified Pisarenko harmonic decomposer (PHD),[13] which calculates the coarse estimate $\hat{\omega}_0^c$ as

$$\hat{\omega}_0^c = \cos^{-1}\left(\frac{d+\sqrt{d^2+8c^2}}{4c}\right), \tag{6}$$

where $d = \sum_{k=5}^{K} r(k-2)[r(k)+r(k-4)]$ and $c = \sum_{k=4}^{K-1} r(k-1)[r(k)+r(k-2)]$. The difference to Ref. 13 is that we set $r(k) = \sum_{n=K+1}^{N-K} x(n)[x(n+k)+x(n-k)]$, $k = 1, 2, 3, \ldots, K$, and $K = round(N/3)$, where $round(x)$ means to round x up or down to the nearest integer. This is to enhance the signal-to-noise ratio (SNR) according to the LP, and the value of K is determined through simulations. Unlike the widely used FFT, the adopted coarse estimator does not suffer from resolution loss for short signal lengths.

B. Spectrum matching

Since most of the values of $S_{m-}(k)$ are forced to approximate zero after modulation, then the key problem is to deal with the interference for $k = 0$. From (4), we know that

$$S_{m+}(0) = \frac{A}{2} e^{j\theta} e^{j\frac{N-1}{2}(\omega_0+\omega_c)} \frac{\sin((\omega_0+\omega_c)N/2)}{\sin((\omega_0+\omega_c)/2)}. \tag{7}$$

According to (3) and (4), for arbitrary value of integer q ($0 < q \le N-1$), we can write

$$\begin{aligned} S_{m+}(q) &= X_m(q) - S_{m-}(q) - W_m(q) \\ &= \frac{A}{2} e^{j\theta} e^{j\frac{N-1}{2}(\omega_0+\omega_c-\tilde{\omega}_q)} \frac{\sin((\omega_0+\omega_c-\tilde{\omega}_q)N/2)}{\sin((\omega_0+\omega_c-\tilde{\omega}_q)/2)}. \end{aligned} \tag{8}$$

Then, substitute (8) for $(A/2)e^{j\theta}$ into (7) and we obtain

$$\begin{aligned} S_{m+}(0) &= (-1)^q e^{j\frac{N-1}{2}\tilde{\omega}_q} \frac{\sin((\omega_0+\omega_c-\tilde{\omega}_q)/2)}{\sin((\omega_0+\omega_c)/2)} \\ &\quad \times (X_m(q) - S_{m-}(q) - W_m(q)). \end{aligned} \tag{9}$$

Thus, substituting $\hat{\omega}_0^c$ for ω_0 and ω_c in (9), we can define an estimator of $S_{m+}(0)$ as

$$\hat{S}_{m+}(0) = (-1)^q e^{j\frac{N-1}{2}\tilde{\omega}_q} \frac{\sin(\hat{\omega}_0^c - \tilde{\omega}_q/2)}{\sin(\hat{\omega}_0^c)} X_m(q). \tag{10}$$

Assuming that $|\Delta\omega_0^c|$ is sufficiently small, it is easy to make the approximation to

$$\frac{\sin(\hat{\omega}_0^c - \tilde{\omega}_q/2)}{\sin(\hat{\omega}_0^c)} \approx \frac{\sin((\omega_0+\omega_c-\tilde{\omega}_q)/2)}{\sin((\omega_0+\omega_c)/2)}. \tag{11}$$

Then we can rewrite (9) as

$$\hat{S}_{m+}(0) = S_{m+}(0) + \varepsilon(q) + \upsilon(q), \tag{12}$$

where $\varepsilon(q)$ and $\upsilon(q)$ can be regarded as the terms of the estimation error caused by $S_{m-}(q)$ and the modulated noise

$$\varepsilon(q) = (-1)^q e^{j\frac{N-1}{2}\tilde{\omega}_q} \frac{\sin((\omega_0+\omega_c-\tilde{\omega}_q)/2)}{\sin((\omega_0+\omega_c)/2)} S_{m-}(q), \tag{13}$$

$$\upsilon(q) = (-1)^q e^{j\frac{N-1}{2}\tilde{\omega}_q} \frac{\sin((\omega_0+\omega_c-\tilde{\omega}_q)/2)}{\sin((\omega_0+\omega_c)/2)} W_m(q). \tag{14}$$

Substitute (5) and $\omega_c = \hat{\omega}_0^c = \omega_0 + \Delta\omega_0^c$ into (13), and as $|\Delta\omega_0^c|$ is assumed to be sufficiently small, so

$$\varepsilon(q) \approx \frac{A\sin(\Delta\omega_0^c N/2)}{2} e^{-j\theta} e^{j\frac{N-1}{2}\Delta\omega_0^c} (\cot(\omega_0) - \cot(\tilde{\omega}_q/2)). \tag{15}$$

Note that q can be an arbitrary integer from 1 to $N-1$, and we can set $\tilde{\omega}_q/2 \to \omega_0$ to make $\varepsilon(q) \to 0$. So q can be approximated by setting $q = round(N\hat{\omega}_0^c/\pi)$. Furthermore, as we assumed that $\Delta\omega_0^c N$ is small in (5), the value of $\varepsilon(q)$ can be sufficiently small to be ignored.

For $\upsilon(q)$, it is easy to prove that $\mathrm{E}[\upsilon(q)] = 0$, where $\mathrm{E}[\cdot]$ is the expectation operator. Then, from (12), we can write

$$\mathrm{E}[\hat{S}_{m+}(0)] = S_{m+}(0) + \varepsilon(q) + \mathrm{E}[\upsilon(q)] \approx S_{m+}(0), \tag{16}$$

which means that $\hat{S}_{m+}(0)$ can be recognized as an unbiased estimator of $S_{m+}(0)$.

Now, we can divide the spectrum of the modulated real signal as $X_m(k)$ into two spectra of complex exponentials, as $\hat{S}_{m+}(k)$ and $\hat{S}_{m-}(k)$, written as

$$\begin{cases} \hat{S}_{m+}(k) = X_m(k) - (X_m(0) - \hat{S}_{m+}(0))\delta(k) \\ \hat{S}_{m-}(k) = (X_m(0) - \hat{S}_{m+}(0))\delta(k) \end{cases}, \quad k = 0, 1, 2, \ldots, N-1, \tag{17}$$

where $\delta(k)$ is the discrete Dirac delta function with $\delta(0) = 1$ and $\delta(k) = 0$ for $k \ne 0$. $X_m(0)$ can be calculated by summing the elements of $x_m(n)$. After this spectrum matching process, the signal amplitude and the initial phase can be directly estimated from $\hat{S}_{m-}(k)$ as $\hat{A} = 2|\hat{S}_{m-}(0)|/N$ and $\hat{\theta} = -angle(\hat{S}_{m-}(0))$, but here we focus on frequency estimation, which can be further derived from $\hat{S}_{m+}(k)$.

C. Error correction

After modulation, the actual frequency of the positive frequency exponential in (2) has been shifted to $\omega_0 + \omega_c$. Accordingly, we can use $2\hat{\omega}_0^c$ to approximately locate the spectral maximum of $S_{m+}(k)$, which is only $\Delta\omega_0^c$ radians per sample distant from the actual value. Then, we could estimate $\Delta\omega_0^c$ to correct the estimation bias of $\hat{\omega}_0^c$. According to the classical methodology of interpolation in the frequency domain,[12,14] we can use two spectral points as $S_{m+}(2\hat{\omega}_0^c - \pi/N)$ and $S_{m+}(2\hat{\omega}_0^c + \pi/N)$ to realize accurate error correction.

From (4), we can calculate $S_{m+}(2\hat{\omega}_0^c - \pi/N)$, $S_{m+}(2\hat{\omega}_0^c + \pi/N)$, and after some simple algebra, we obtain

$$\begin{aligned} &\left(\sin\left(\frac{\pi}{2N}\right)\cos\left(\frac{\Delta\omega_0^c}{2}\right) - \cos\left(\frac{\pi}{2N}\right)\sin\left(\frac{\Delta\omega_0^c}{2}\right)\right) S_{m+}\left(2\hat{\omega}_0^c - \frac{\pi}{N}\right) e^{-j\frac{N-1}{N}\cdot\frac{\pi}{2}} \\ &\quad = \frac{A}{2} e^{j\theta} e^{-j\frac{N-1}{2}\Delta\omega_0^c} \cos\left(\frac{N\Delta\omega_0^c}{2}\right), \end{aligned} \tag{18}$$

$$\begin{aligned} &\left(\sin\left(\frac{\pi}{2N}\right)\cos\left(\frac{\Delta\omega_0^c}{2}\right) + \cos\left(\frac{\pi}{2N}\right)\sin\left(\frac{\Delta\omega_0^c}{2}\right)\right) S_{m+}\left(2\hat{\omega}_0^c + \frac{\pi}{N}\right) e^{j\frac{N-1}{N}\cdot\frac{\pi}{2}} \\ &\quad = \frac{A}{2} e^{j\theta} e^{-j\frac{N-1}{2}\Delta\omega_0^c} \cos\left(\frac{N\Delta\omega_0^c}{2}\right). \end{aligned} \tag{19}$$

By subtracting the both sides of (18) and (19), making $\exp(j(N-1)\pi/N) \approx -1$ and $\tan(x) = x$ for sufficiently small x, after some simplification, we obtain

$$\left(\Delta\omega_0^c - \frac{\pi}{N}\right) S_{m+}\left(2\hat{\omega}_0^c - \frac{\pi}{N}\right) = \left(\Delta\omega_0^c + \frac{\pi}{N}\right) S_{m+}\left(2\hat{\omega}_0^c + \frac{\pi}{N}\right). \tag{20}$$

Substitute $\hat{S}_{m+}(2\hat{\omega}_0^c - \pi/N)$, $\hat{S}_{m+}(2\hat{\omega}_0^c + \pi/N)$ for $S_{m+}(2\hat{\omega}_0^c - \pi/N)$ and $S_{m+}(2\hat{\omega}_0^c + \pi/N)$ and take the real part to avoid complex value. We can estimate $\Delta\omega_0^c$ as

$$\Delta\hat{\omega}_0^c = \frac{\pi}{N} \mathrm{Re}\left[\frac{\hat{S}_{m+}(2\hat{\omega}_0^c + \pi/N) + \hat{S}_{m+}(2\hat{\omega}_0^c - \pi/N)}{\hat{S}_{m+}(2\hat{\omega}_0^c - \pi/N) - \hat{S}_{m+}(2\hat{\omega}_0^c + \pi/N)}\right], \tag{21}$$

where $\hat{S}_{m+}(2\hat{\omega}_0^c \pm \pi/N)$ can be calculated from the inverse DFT of $\hat{S}_{m+}(k)$ in (17) as

TABLE I. Signal processing algorithm.

1	Calculate the coarse frequency estimate $\hat{\omega}_0^c$ via (6).
2	Modulate $x(n)$ with $\omega_c = \hat{\omega}_0^c$ to obtain $x_m(n)$ as in (2).
3	Calculate $q = round(N\hat{\omega}_0^c/\pi)$ and $X_m(q) = \sum_{n=0}^{N-1} x_m(n)e^{-j\tilde{\omega}_q n}$.
4	Calculate $\hat{S}_{m+}(0)$ according to (10).
5	Calculate $\hat{S}_{m+}(2\hat{\omega}_0^c + \pi/N)$ and $\hat{S}_{m+}(2\hat{\omega}_0^c - \pi/N)$ via (22)
6	Generate the frequency correction factor $\Delta\hat{\omega}_0^c$ via (21).
7	Obtain the fine frequency estimate by $\hat{\omega}_0^f = \hat{\omega}_0^c - \Delta\hat{\omega}_0^c$.

$$\hat{S}_{m+}(2\hat{\omega}_0^c \pm \pi/N) = \sum_{n=0}^{N-1}\left[x_m(n) - \left(X_m(0) - \hat{S}_{m+}(0)\right)/N\right]e^{-j(2\hat{\omega}_0^c \pm \pi/N)n}. \tag{22}$$

Finally, the fine frequency estimate ($\hat{\omega}_0^f$) of our method can be calculated by $\hat{\omega}_0^f = \hat{\omega}_0^c - \Delta\hat{\omega}_0^c$. The overall signal processing algorithm for the proposed method is shown in Table I.

IV. SIMULATION RESULTS

To evaluate the performance of the aforementioned two-step methods, we use the TSA,[7] EA,[8] PM,[9] and PCA[10] methods as a comparison against our proposed method. Without loss of generality, we assume $A = 1$ and θ is uniformly distributed between $-\pi$ and π. Each simulation result is carried out with an average of 2000 independent Monte Carlo runs.

A. Bounds

As with the approximation made in Ref. 15, the CRLB of frequency estimation for a real sinusoid is given as

$$\text{CRLB} = \text{var}[\hat{\omega}_0^f] = \frac{12}{\text{SNR} \cdot N(N^2 - 1)}, \tag{23}$$

where the SNR is defined as $A^2/(2\sigma^2)$.

B. Variable frequency

Because of the periodicity of the spectrum of a real sinusoid, we only evaluate the performance for $0 \le \omega_0 \le 0.5\pi$. The root-mean-square error (RMSE) vs signal frequency ω_0 for $N = 32$ for four different SNR values is presented in Fig. 2. The signal frequency varies from 0.01π to 0.49π with a step size of 0.01π. The enlarged scale of $1.5\pi \le \omega_0 \le 3.5\pi$ can show the advantages of the proposed method more clearly. When the signal frequency is very low, the PCA and EA methods provide more reliable accuracy at SNR = 10 dB in Fig. 2(a), while the PM method performs better for high SNRs in Figs. 2(c) and 2(d). However, generally speaking, the proposed method shows higher accuracy than the other evaluated methods in a very large range of signal frequencies, and the superiority becomes more obvious with increasing SNRs.

C. Variable SNR

The RMSE vs SNR for $\omega_0 = 0.09\pi$ and $N = 32$ is shown in Fig. 3. The SNR varies from −10 dB to 119 dB with a step size

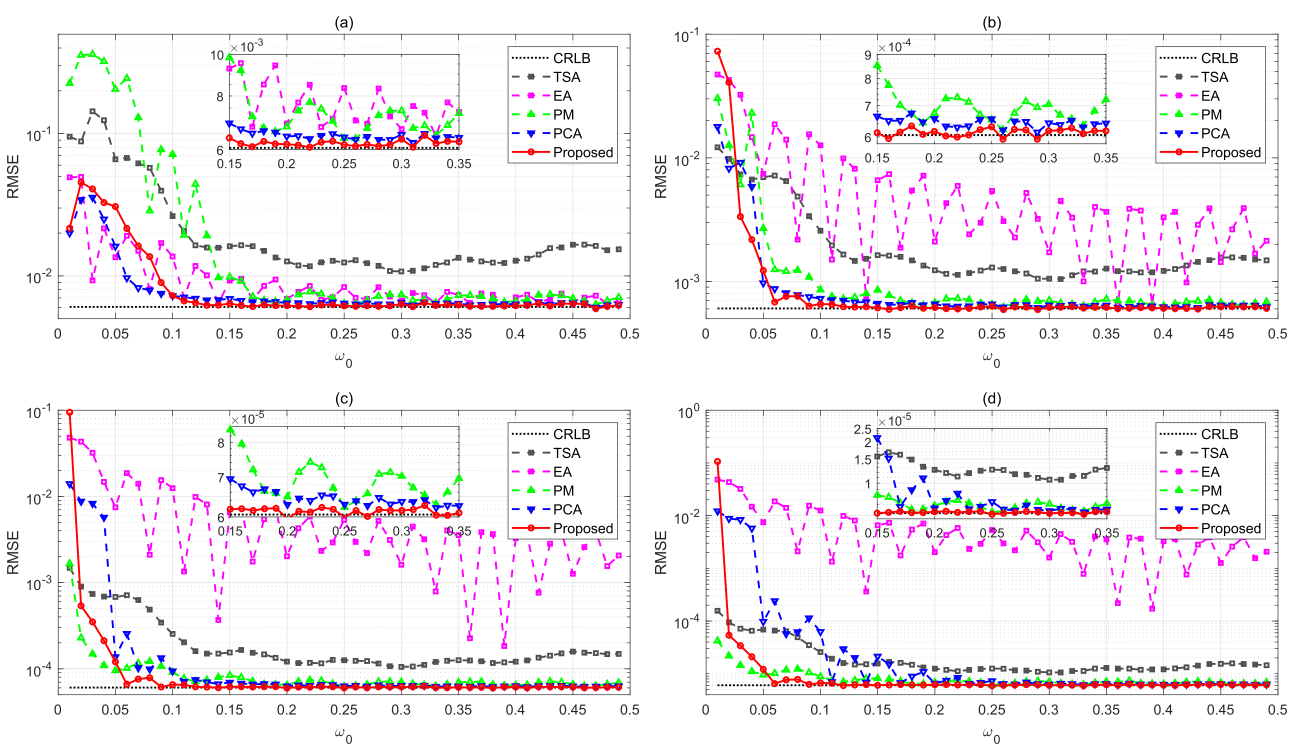

FIG. 2. RMSE vs ω_0 for N = 32. SNR = 10 dB (a), 30 dB (b), 50 dB (c), and 70 dB (d).

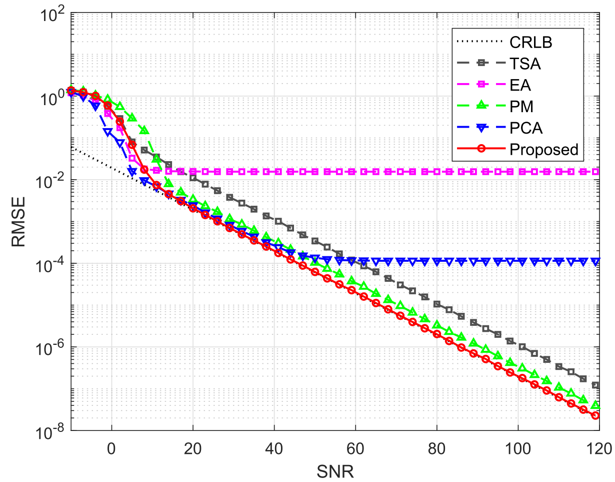

FIG. 3. RMSE vs SNR for $\omega_0 = 0.09\pi$ and $N = 32$.

of 3 dB. The effect of RMSE saturation can be found for the EA and PCA methods, which has proved their biasness in this case. By contrast, the TSA, PM, and proposed methods can follow the trend of the CRLB without error floors, but only the proposed method can asymptotically approach the CRLB for sufficiently large SNRs.

D. Variable signal length

The RMSE vs signal length for $\omega_0 = 0.09\pi$ for two SNR values is presented in Fig. 4. The reformed signal length $\log_2 N$ continuously increases from 5 to 12 (32–4096 for N). For two SNR values of 30 dB and 70 dB, evident advantages of the proposed method can be found for short signal lengths (e.g., $N < 128$). With increasing the signal length, all the TSA, PM, PCA and the proposed methods can closely follow the CRLB. However, from the enlarged subgraph, we can see that the proposed method is even slightly better than the other evaluated methods.

E. Computational complexity

The result of the comparison of computational complexity is shown in Table II. All the complex-valued (CV) operations are converted to real-valued (RV) additions and multiplications, following the principle listed on the right-hand part of Table II. We neglect all the computations with $O(1)$ complexity. To make the comparison more clearly, the amount of required additions and multiplications for the evaluated methods is shown in Fig. 5. The signal length N varies from 10 to 500 with a step size of 10. Obviously, we can see

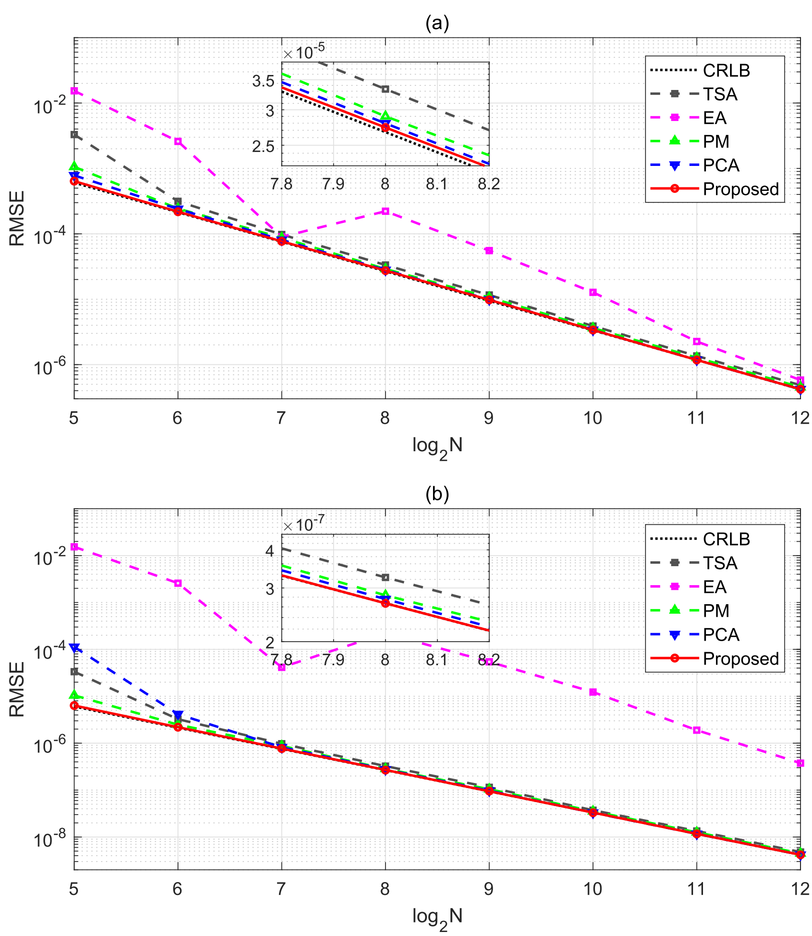

FIG. 4. RMSE vs $\log_2 N$ for $\omega_0 = 0.09\pi$. SNR = 30 dB (a) and 70 dB (b).

TABLE II. Comparison of computational complexity. Note: $M_0 = \lfloor (N-1)/2 \rfloor$, $p = 0.46N$, and $M = \lceil \log_2 2N \rceil$, where $\lfloor x \rfloor$ or $\lceil x \rceil$ means to round x down or up to the nearest integer.

			Converting principle		
Method	Addition	Multiplication	Operation	Addition	Multiplication
TSA[7]	$2NM_0^2 + M_0^2 - 8M_0^3/3 - 32N$	$NM_0^2 + M_0^2 - 4M_0^3/3 - 26M_0/3 - 16N$	CV × CV	2	4
EA[8]	$5N^2/18 - 5N/2$	$5N^2/18 - 3N/2$	CV × RV	0	2
PM[9]	$2Np - 4p^2 + 8p$	$Np - 2p^2 + 9p$	CV + CV	2	0
PCA[10]	$3M2^{M+1} + 2^{M+1} + 3N$	$M2^{M+2} + 2^{M+2} + 41N/3$	CV + RV	1	0
Proposed	$2N^2/9 + 51N/3$	$N^2/9 + 56N/3$			

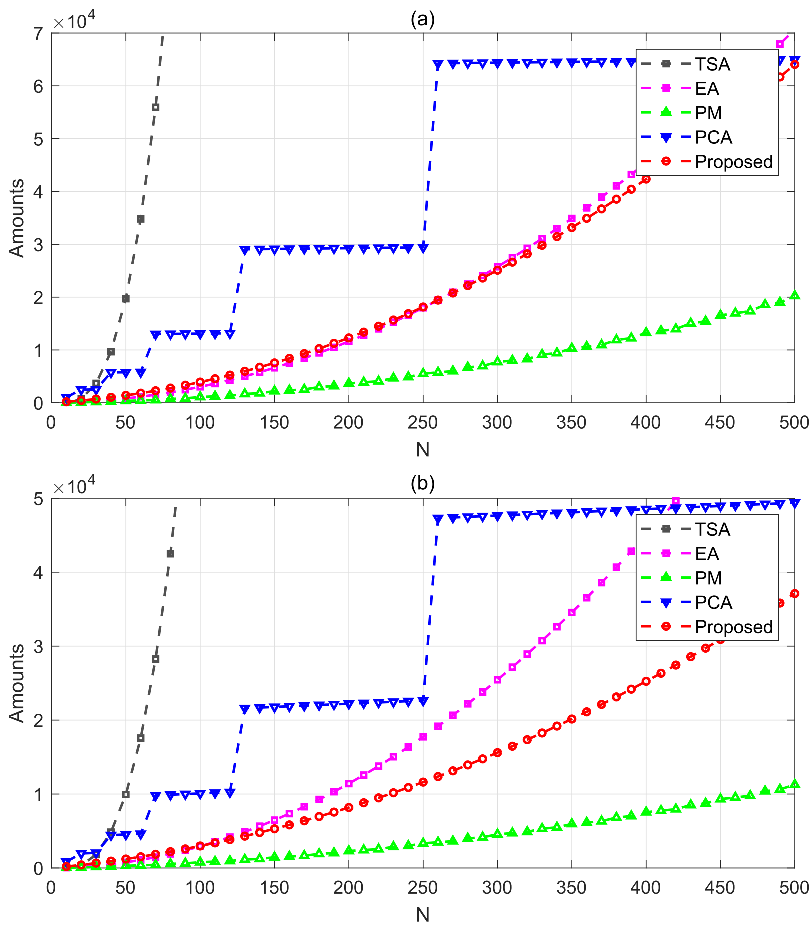

FIG. 5. Amounts of (a) additions and (b) multiplications vs *N*.

that the computational complexity of the proposed method is only higher than the PM method, while the TSA, EA, and PCA methods require more additions and multiplications within the simulated scale of signal lengths.

V. CONCLUSION

In this paper, we put emphasis on dealing with incoherent sampling, which is admittedly a problematic factor in the frequency estimation of sinusoids. According to some earlier studies, we can use a coarse frequency estimate to further generate a correction factor, so as to remove the estimation error introduced by incoherent sampling. In addition to the LS principle based algorithm and its modified versions in the aforementioned studies,[8–10] we proposed a spectrum matching based method to generate the correction factor. In comparison with four other methods, the proposed method shows better performance in simulations, particularly when the signal lengths are short. The computational complexity of our method is also reasonable through the analysis. As long as the SNR reaches a certain level, the proposed method can closely approach the CRLB without any error floor, which means that the proposed method can be very useful in some high SNR applications such as measurement and instrumentation. In addition, the proposed spectrum matching process can be also used for the estimation of the signal amplitude and initial phase. For further study, the estimation accuracy for an extremely small value of the signal frequency would be concerned.

ACKNOWLEDGMENTS

This study was supported by the National Natural Science Foundation of China (NNSFC) (Grant No. 61871402), the Postgraduate Research Innovation Project of Chongqing (CYB14100), the Natural Science Foundation of Tianjin (Grant No. 18JCQNJC01400), the Key Program of Natural Science Foundation of Chongqing (Grant No. cstc2015 jcyjBX0017), the Ph.D. Startup Foundation (WHB201707), and the Special Project for 100 Academic and Discipline Talents of Chongqing (2012-44).

REFERENCES

[1] D. C. Rife and R. R. Boorstyn, "Single tone parameter estimation from discrete-time observations," IEEE Trans. Inf. Theory **20**, 591–598 (1974).
[2] E. Jacobsen and P. Kootsookos, "Fast, accurate frequency estimators," IEEE Signal Process. Mag. **24**, 123–125 (2007).
[3] C. Candan, "A method for fine resolution frequency estimation from three DFT samples," IEEE Signal Process. Lett. **18**, 351–354 (2011).
[4] C. Candan, "Fine resolution frequency estimation from three DFT samples: Case of windowed data," Signal Process. **114**, 245–250 (2015).
[5] S. Ye, J. Sun, and E. Aboutanios, "On the estimation of the parameters of a real sinusoid in noise," IEEE Signal Process. Lett. **24**, 638–642 (2017).
[6] S. Djukanović, "An accurate method for frequency estimation of a real sinusoid," IEEE Signal Process. Lett. **23**, 915–918 (2016).
[7] K. W. K. Lui and H. C. So, "Two-stage autocorrelation approach for accurate single sinusoidal frequency estimation," Signal Process. **88**, 1852–1857 (2008).
[8] Y. Cao, G. Wei, and F.-J. Chen, "A closed-form expanded autocorrelation method for frequency estimation of a sinusoid," Signal Process. **92**, 885–892 (2012).
[9] Y. Shen, Y. Tu, L. Chen, and T. Shen, "A phase match based frequency estimation method for sinusoidal signals," Rev. Sci. Instrum. **86**, 045101 (2015).
[10] Y. Tu and Y. Shen, "Phase correction autocorrelation-based frequency estimation method for sinusoidal signal," Signal Process. **130**, 183–189 (2016).
[11] K. Wang, Y. Tu, Y. Shen, and W. Xiao, "A modulation based phase difference estimator for real sinusoids to compensate for incoherent sampling," Rev. Sci. Instrum. **89**, 085120 (2018).
[12] E. Aboutanios and B. Mulgrew, "Iterative frequency estimation by interpolation on Fourier coefficients," IEEE Trans. Signal Process. **53**, 1237–1242 (2005).
[13] K. W. K. Lui and H. Cheung So, "Modified Pisarenko harmonic decomposition for single-tone frequency estimation," IEEE Trans. Signal Process. **56**, 3351–3356 (2008).
[14] L. Fan and G. Qi, "Frequency estimator of sinusoid based on interpolation of three DFT spectral lines," Signal Process. **144**, 52–60 (2017).
[15] M. Kay Steven, *Fundamentals of Statistical Signal Processing, Volume I: Estimation Theory* (Prentice-Hall, Upper Saddle River, NJ, USA, 1993).